25th ABCM International Congress of Mechanical Engineering
October 20-25, 2019, Uberlândia, MG, Brazil

# COB-2019-0955
# PARAMETER ESTIMATION DURING THE HEATING AND THERMAL DECOMPOSITION OF BIOLOGICAL TISSUES

**Bruna Rafaella Loiola**
Instituto Militar de Engenharia, IME
bruna.loiola@ime.eb.br

**Luiz Alberto da Silva Abreu**
Universidade Estadual do Rio de Janeiro, UERJ
luiz.abreu@uerj.br

**Helcio Rangel Barreto Orlande**
Universidade Federal do Rio de Janeiro, UFRJ
helcio@mecanica.coppe.ufrj.br

***Abstract.*** *The objective of this work was to estimate the parameters of the mathematical model used to represent the heating of a biological tissue. A sample of bovine muscle was used for the experiments. The tissue was heated with an electrical radiator, while its surface temperature was measured with an infrared camera. The imposed heat flux was estimated with a sample of Plexiglas, with known thermophysical properties. The Markov Chain Monte Carlo method and an Approximate Bayesian Computation algorithm were used for the solutions of the inverse problems examined in this work. The agreement of measured and estimated temperatures was excellent, thus demonstrating that the model and the estimated parameters appropriately represent the physics of the experiment.*

***Keywords:*** *heat transfer, biological tissues, experimental data, numerical solution*

## 1. INTRODUCTION

Burn injuries are critical in applications ranging from medicine to defense (Atiyeh et al., 2007; Abraham et al., 2016; Abraham et al, 2018). The burns can be associated to the thermal decomposition of the affected tissues and have been studied by several research groups since the seminal works of Henriques and Moritz (Henriques, 1947; Moritz, 1947; Henriques and Moritz, 1947; Moritz and Henriques, 1947). In general, thermal damage is related to the temperature increase of the tissue due to an external heat source. The bioheat equation proposed by Pennes (1948) that accounts for blood perfusion is still the model mostly used to describe heat transfer in tissues. However, for *in-vitro* or *ex-vivo* experiments, blood perfusion and metabolic heat generation do not take place and Pennes' model reduces to the heat conduction equation. Nevertheless, the thermal properties of biological tissues depend on their composition and temperature (Valvano, 2011; Valvano 2018). In this context, the goal of this work is to numerically reproduce measurements of the temperature at the top and bottom surfaces of a biological tissue, externally heated by radiation. Moreover, the thermal damage parameters of an Arrhenius model were calibrated with an intrusive measurement of the thermal decomposition front inside the tissue.

## 2. EXPERIMENTAL SETUP

The experiments were performed in the Laboratory of Heat Transfer and Technology (LTTC) of the Federal University of Rio de Janeiro. A sample of bovine muscle was heated by a transient uniform heat flux provided by an electrical radiator, as illustrated in Fig. 1a. The environment temperature was measured with a digital thermo-hygrometer MINIPA MTH-1380. The temperature at the bottom surface of the sample was measured with two type E thermocouples connected to an Agilent 34970-A acquisition system. The temperature distribution at the sample surface was measured with an infrared camera, model FLIR SC 660, by using a desktop computer compatible with FLIR ResearchIR™ software for data acquisition, as shown by Fig. 1a. Figure 1b illustrates a similar experiment performed with a Plexiglas plate with known thermal properties, in order to estimate the transient heat flux at the upper surface of the sample.

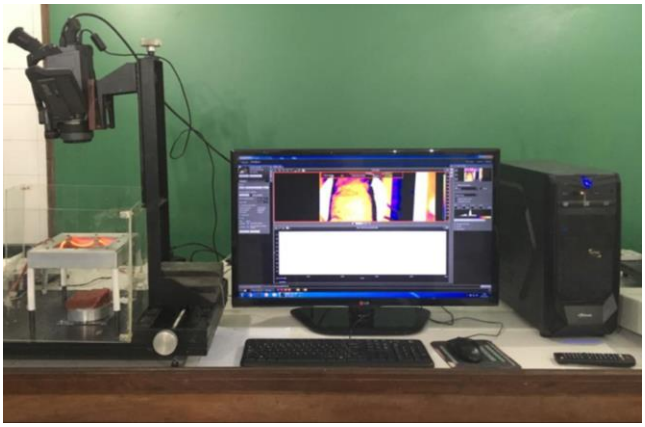

(a)

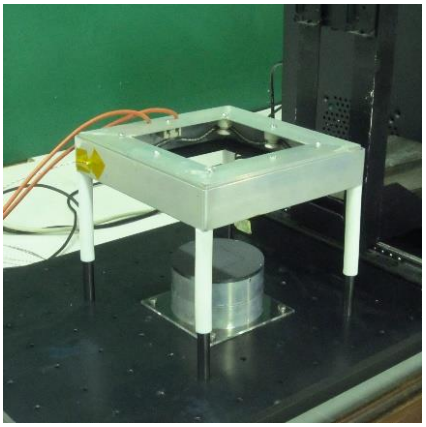

(b)

Figure 1. a) Electrical systems of heating and Equipment used to data acquisition; b) Heating of a Plexiglas plate.

The experiment was performed with a bovine muscle sample of 32 mm of thickness (*H*), heated during 3570 s by the electrical radiator, with a voltage of 100 V. The environment temperature was 22.6 °C with a relativity humidity of 71.5 %. The initial temperature of the sample at the top surface was measured with the infrared camera as 21.73°C, while at the bottom surface the thermocouple measurements with the two thermocouples were 22.3°C.

In order to estimate the transient heat flux applied to the surface of the tissue, a similar experiment was performed with a Plexiglas plate with known thermal properties and geometry, as presented by Tab. 1. In this experiment, care was taken to maintain the same distance from the upper surface of the sample to the radiator.

Table 1. Plexiglas plate properties and geometry (Abreu et al., 2018).

| Plexiglas Properties | Value | Geometry of the plate | Value |
|---|---|---|---|
| Thermal conductivity [W/(m.K)] | 0.22 | Thickness [mm] | 2 |
| Specific heat [J/(kg.K)] | 1450 | Width [mm] | 40 |
| Density [kg/m³] | 1150 | Length [mm] | 40 |

## 3. PHISICAL PROBLEM AND MATHEMATICAL FORMULATION

The physical problem involving the heating of the biological tissue was considered one-dimensional, in Cartesian coordinates. The heat flux imposed over the top surface of the sample was assumed as uniform. Heat losses to the surrounding environment by convection and linearized radiation at the top surface were accounted for by Newton's law, with a heat transfer coefficient $h_\infty$ and environment temperature $T_\infty$. Heat losses through the bottom surface were also considered by Newton's law with a coefficient *U* that represents the global heat transfer coefficient through the support system below the sample. Water loss at the heated surface by evaporation was neglected. Similarly, the variations of thermal properties with temperature and water content were not considered. Instead, the sample thermal conductivity was considered varying along the sample's thickness, while the volumetric heat capacity was considered constant, C = 3075.6 kJ/(m³.K). The sample is assumed initially with a non-uniform temperature, $T_0(z)$. The mathematical formulation for the physical problem is given by:

$$C\frac{\partial T(z,t)}{\partial t} = \nabla \cdot [k(z)\nabla T(z,t)] \qquad 0 < z < H \qquad t > 0 \qquad (1)$$

$$T(z,t) = T_0(z) \qquad 0 \le z \le H \qquad t = 0 \qquad (2)$$

$$-k(z)\frac{\partial T(z,t)}{\partial z} + UT(z,t) = UT_\infty \qquad z = 0 \qquad t > 0 \qquad (3)$$

$$-k(z)\frac{\partial T(z,t)}{\partial z} - h_\infty T(z,t) = -h_\infty T_\infty - q_u(t) \qquad z = H \qquad t > 0 \qquad (4)$$

In these equations, *C* indicates the volumetric heat capacity and *k* is the thermal conductivity. The longitudinal direction is represented by *z* and time by *t*. The heat flux $q_u$ is imposed by an electrical radiator at the upper surface of the sample with a thickness *H*. The information about the transient heat flux was provided by a second experiment performed with a Plexiglas sample with known properties. The initial temperature of the sample was considered with a linear variation along the sample's length *H*, as indicated by Eq. (5). The information about the temperature of the top

surface ($T_u$) was provided by the thermal camera while the temperature of the bottom surface ($T_b$) was given by the type E thermocouple, at the initial time.

$$T_0(z) = (T_u - T_b)\frac{z}{H} + T_b \tag{5}$$

The thermal conductivity was considered as linear function of the position, that is,

$$k(z) = k_0 + k_1 z \tag{6}$$

The information about surface temperatures were used to estimate the parameters $k_0$, $k_1$, $h_\infty$ and $U$ through inverse analysis. The Arrhenius thermal damage formulation, given by Eq. (7), was used in order to estimate the thermal damage decomposition, represented by $\Omega$. The parameter $\gamma$ is the exponent of the scale factor, the parameter $E_a$ is the activation energy and $R$ is the universal gas constant (8.314 J mol$^{-1}$K$^{-1}$). The criterion of $\Omega \geq 1$ was used to define the thermal decomposition region.

$$\Omega = \int_0^t 10^{\gamma} e^{\left[-\frac{E_a}{RT}\right]} dt' \tag{7}$$

## 4. NUMERICAL SOLUTION

The numerical simulations were performed within the MATLAB® platform. The solution of the direct problem given by Eqs. (1) to (4) was obtained with the Finite Volume Method (Patankar, 1980; Ozisik et al., 2017). The heat flux ($q_u$) imposed by the radiator was estimated with the Markov chain Monte Carlo (MCMC) method, with the temperature measurements obtained over the surface of the Plexiglas plate. Afterwards, the MCMC Method was used to estimate the parameters of the forward problem, $k_0$, $k_1$, $h_\infty$ and $U$, by using the Metropolis-Hastings algorithm (Metropolis et al., 1953; Hastings, 1970) presented by Tab. 2.

Table 2. Metropolis-Hastings algorithm (Metropolis et al., 1953; Hastings, 1970).

1. Start the chain at $\mathbf{P}^j$
2. Sample $\mathbf{P}^*$ from $\pi(\mathbf{P}^*|\mathbf{P}^j)$
3. Calculate of the acceptance probability of the movement
$$\alpha = min\left\{1, \frac{\pi(\mathbf{P}^*|\mathbf{Y})\pi(\mathbf{P}^j|\mathbf{P}^*)}{\pi(\mathbf{P}^j|\mathbf{Y})\pi(\mathbf{P}^*|\mathbf{P}^j)}\right\}$$
4. Sample u from uniform distribution U (0,1).
5. If $\alpha \geq$ u, accept $\mathbf{P}^*$ and do $\mathbf{P}^{j+1} = \mathbf{P}^*$. Otherwise, reject $\mathbf{P}^*$ and do $\mathbf{P}^{j+1} = \mathbf{P}^j$.
6. Return to step 2 and repeat the process until convergence of the chain and properly posteriori distribution of $\pi(\mathbf{P}|\mathbf{Y})$.

The vector of parameters is represented by $\mathbf{P}$ while the vector of measurements is represented by $\mathbf{Y}$. The priori assumed for the parameters is given by $\pi(\mathbf{P})$. In this algorithm, a candidate $\mathbf{P}^*$ is sample from a proposal $\pi(\mathbf{P}^*|\mathbf{P}^j)$ at each state $j$. The choice of the proposal is fundamental for the implementation of the Metropolis-Hastings algorithm, since the objective density $\pi(\mathbf{P}|\mathbf{Y})$ depends of the chain's movement. In this work, the proposal is considered as a uniform U (-1,1) random walk model ($r_w$) around the current value of the chain $\mathbf{P}^j$, as follow:

$$P^* = P^j + r_w U(-1,1) \tag{8}$$

The priors adopted for the parameters are uniform distributions, while the likelihood is considered as a Gaussian distribution. In this case, the acceptance ratio is only dependent of the likelihood, as follows:

$$\alpha = min\left\{1, \frac{\pi(\mathbf{P}^*|\mathbf{Y})}{\pi(\mathbf{P}^j|\mathbf{Y})}\right\} \tag{9}$$

The Approximate Bayesian Computation (ABC) was used to calibrate the parameters of the Arrhenius thermal damage model through the algorithm of Toni et al. (2009), given by Tab. 3. In this algorithm, specified tolerances are defined at the begin of the simulation to converge the intermediate distributions. A particle $\mathbf{P}^{**}$, defined as a set of parameters, is sampled from the priori $\pi(\mathbf{P})$. The direct problem $f(\mathbf{Y}|\mathbf{P}^{**})$ is then solved and a candidate $\mathbf{Y}^*$ is obtained. If the distance between the candidate and the measurements is less than the specified tolerance ($d \leq \varepsilon$), the candidate $\mathbf{Y}^*$ is accepted. This process of sampling the particle is repeated until $N$ particles are accepted. For the population (set of accepted particles), the weights are calculated and normalized for each particle. From the previous population, samples

are generated by resampling according to the weights to generate $\mathbf{P}^*$ and these particles are perturbed with a Kernel transition in order to obtain $\mathbf{P}^{**}$. After the new population is obtained, the weights are calculated and normalized and this process is solved until the last tolerance $\varepsilon_p$ based on Morozov's discrepancy principle is reached.

Table 3. ABC SMC - algorithm of Toni et al. (2009).

**1.** Define the tolerances $\varepsilon_1, \varepsilon_2, \ldots, \varepsilon_p$ for each of the iterations (populations) used for selecting the parameters. Also, specify the distance function $d(\mathbf{Y},\mathbf{Y}^*)$ that substitutes the likelihood function. Set the population indicator $p = 0$.

**2.** Set the particle indicator $i = 1$, where each particle represents a set of parameters.

**3.** Sample the particle $\mathbf{P}^*$ from the prior distribution for the models $\pi(\mathbf{P})$.

If $p = 0$, sample the candidate parameters $\mathbf{P}^{**}$ from the prior distribution. Else, sample $\mathbf{P}^*$ from the previous population $\mathbf{P}_{p-1}^i$ with weights $\mathbf{w}_{p-1}^i$ and perturb this particle to obtain $\mathbf{P}^{**} \approx K_p(\mathbf{P}^*, \mathbf{P}^{**})$, where $K_p$ is a perturbation kernel.

**4.** If $\pi(\mathbf{P}^{**}) = 0$, return to step 3. Else, simulate from the forward problem (operator $f$) a candidate set of observable variables with parameters $\mathbf{P}^{**}$, that is, $y^* \approx f(\mathbf{Y}|\mathbf{P}^{**})$.

**5.** If $d(\mathbf{Y},\mathbf{Y}^*) > \varepsilon_p$ return to step 3. Otherwise, set $P_p^i = P^{**}$, add $\mathbf{P}^{**}$ and calculate its weight as

$$\mathbf{w}_p^i = \begin{cases} 1\,, & if\ p = 0 \\ \dfrac{\pi\left(\mathbf{P}_p^i\right)}{\sum_{j=1}^{N} \mathbf{w}_{p-1}^j K_p\left(\mathbf{P}_{p-1}^j, \mathbf{P}_p^i\right)}, & if\ p > 0 \end{cases}$$

**6.** If $i < N$, where $N$ is the number of particles, set $i = i + 1$ and go to step 3.

**7.** Normalize the weights.

**8.** If $p < P$, where $P$ is the number of iterations (populations), set $p = p + 1$ and go to step 2. Otherwise, terminate the iterations.

## 5. RESULTS AND DISCUSSION

The Plexiglas plate surface temperature distribution measured with the infrared camera was used in order to estimate the heat flux provided by the radiator, as illustrated in Fig. 2, by using the MCMC method. A Smoothness Gaussian prior was considered with a constant parameter of 1000.

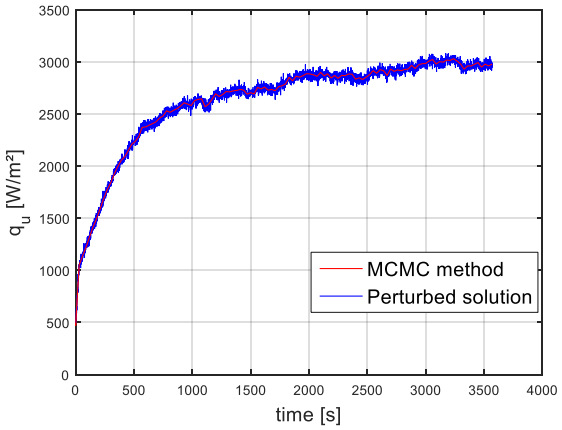


Figure 2. Heat flux at the top surface.

The MCMC method was then used to determinate the thermal conductivity parameters, the heat transfer coefficient and the global coefficient $U$. A uniform prior was adopted for each parameter, as presented by Tab. 4. The chain was started at the middle point of the priors' upper and lower limits. The random walk step for each parameter is also presented by Tab. 4.

Table 4. Priori adopted for the parameters.

| Parameter | Unity | Priori | Initial value | Random walk |
|---|---|---|---|---|
| Thermal conductivity parameter: $k_0$ | [W/(m.K)] | U (0,1) | 0.5 | 0.0001 |
| Thermal conductivity parameter: $k_1$ | [W/(m².K)] | U (-40,40) | 0 | 0.004 |
| Heat transfer coefficient: $h_\infty$ | [W/(m².K)] | U (0,100) | 50 | 0.1 |
| Global coefficient: $U$ | [W/(m².K)] | U (0,100) | 50 | 0.1 |

Chains with 400,000 states were simulated, with an acceptance rate of 18.24%. The Markov chains for the thermal conductivity parameters are presented by Fig. 3, while the chains for the heat transfer coefficients *h* and *U* are presented by Fig. 4.

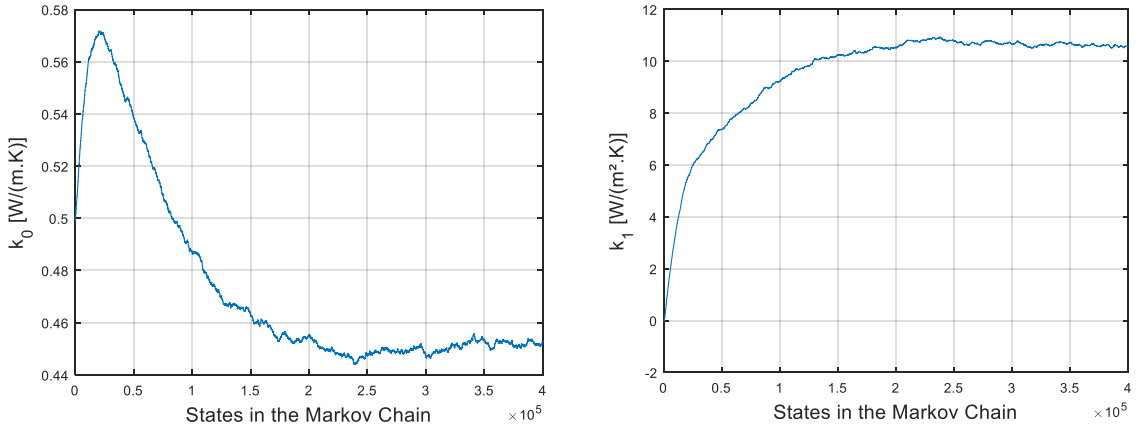


Figure 3. Markov chain to the thermal conductivity parameters: a) $k_0$; b) $k_1$.

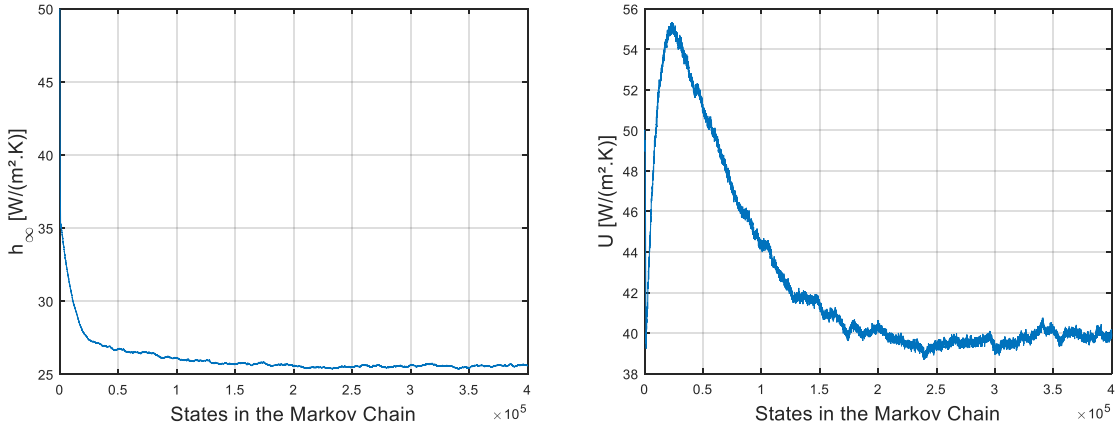


Figure 4. Markov chain: a) $h_\infty$; b) $U$.

The statistics of the estimated parameters are presented by Tab. 5, considering a burn-in period with 300,000 states to reach equilibrium of the chains. The estimated heat transfer coefficient is compatible with natural convection with air. In this work, this coefficient also takes into account the linearized radiation.

The thermal conductivity calculated with the mean parameters of $k_0$ and $k_1$ is presented at Fig. 5a. In Valvano (2011, 2018), the values of thermal conductivities of different biological tissues can be found with a mean value around 0.5 W/(m.K), which increase with temperature. In this sense, the thermal conductivity presented by Fig. 5a is compatible with the literature. The heat flux lost from the bottom surface, illustrated by Fig. 5b, increases with time, since the temperature of the bottom surface increases.

Table 5. Statistics of the estimated parameters.

| Parameter | Mean | Standard deviation | 95% Credibility Interval |
|---|---|---|---|
| $k_0$ [W/(m.K)] | 0.4514 | 0.0018 | 0.4471 – 0.4542 |
| $k_1$ [W/(m².K)] | 10.6246 | 0.0588 | 10.5186 – 10.7393 |
| $h_\infty$ [W/(m².K)] | 25.5671 | 0.0739 | 25.4053 – 25.7057 |
| $U$ [W/(m².K)] | 39.8257 | 0.2888 | 39.2218 – 40.3454 |

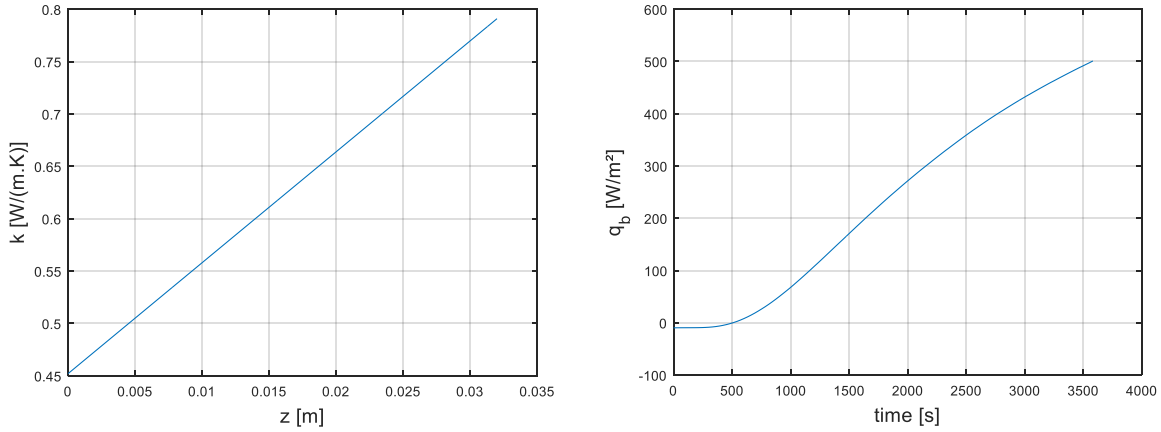


(a) (b)

Figure 5. a) Thermal conductivity; b) Heat flux lost by the bottom surface.

The converged parameters were then used to calculate the temperature distribution of the sample. The numerical temperature of the bottom surface is compared to the experimental measurements in Fig. 6a while the experimental data of the temperature at the top surface of the sample is compared to the numerical solution at Fig. 6b. Both comparisons present good agreements between the numerical and experimental data. The temperature along the tissue at the end of heating is presented at Fig. 6c.

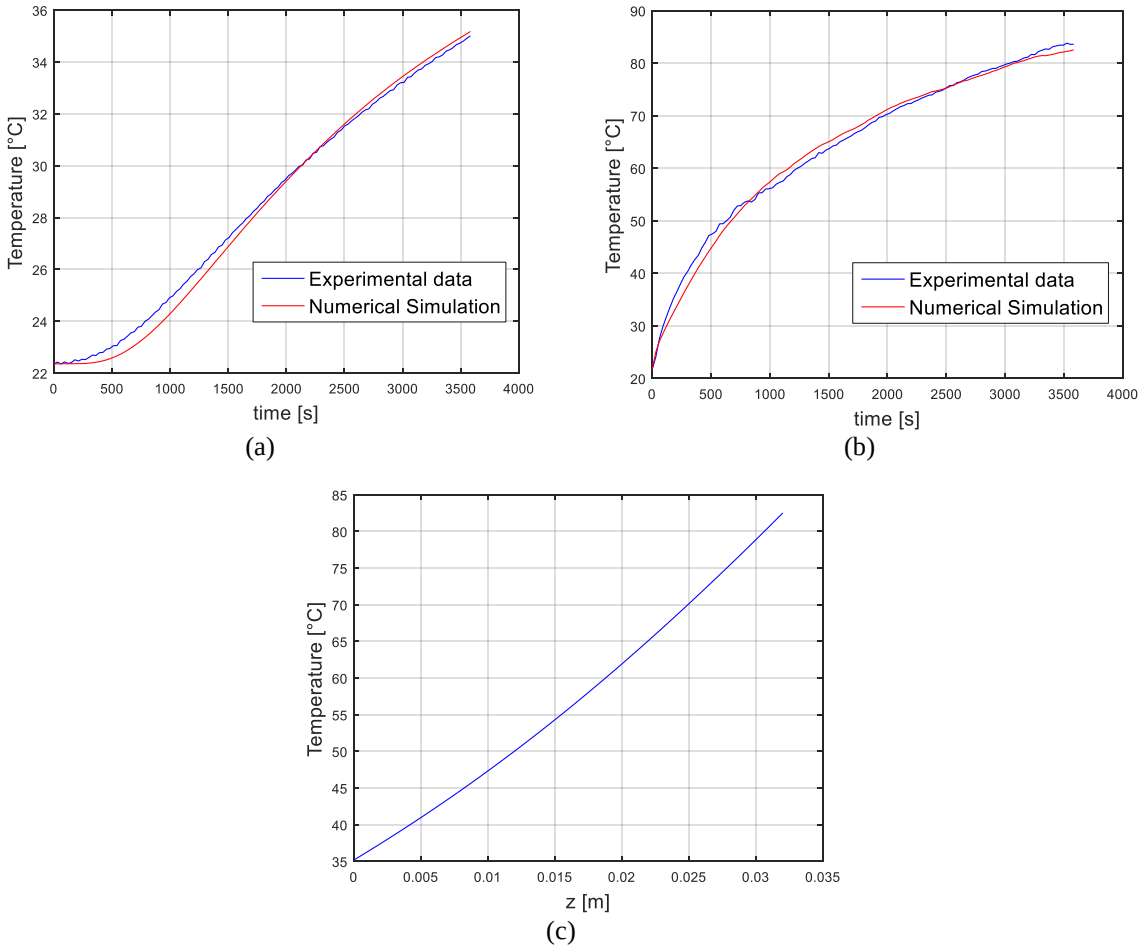


(a) (b)

(c)

Figure 6. Temperatures of the sample at $t$ = 3570 s: a) Bottom surface; b) Upper surface; c) The temperature along the longitudinal direction.

Once the parameters were estimated and the results present good agreement with the experimental data, the calibration of the thermal damage model was assessed. The ABC SMC method with 200 particles was applied in order to calibrate the Arrhenius parameters model for the thermal damage, Eq. (7), considering uniform priors for the parameters, as presented by Tab. 6. The position of the thermal decomposition front measured at $t$ = 3570 s was used to estimate these parameters. The statistics of the estimated thermal decomposition parameters is presented by Tab. 6, and the corresponding histograms of the marginal posterior distributions are presented in Fig. 7.

Table 6. Statistics of the thermal decomposition parameters.

| Parameter | Priori | Transition Kernel | Mean | Standard deviation | 95% Credibility Interval |
|---|---|---|---|---|---|
| $\gamma$ | U (20,100) | U (-3,3) | 63.2526 | 1.4213 | 60.4030 – 66.1911 |
| $E_a$ [kJ/mol] | U (100,900) | U (-10,10) | 434.97 | 9.2034 | 415.57 – 454.47 |

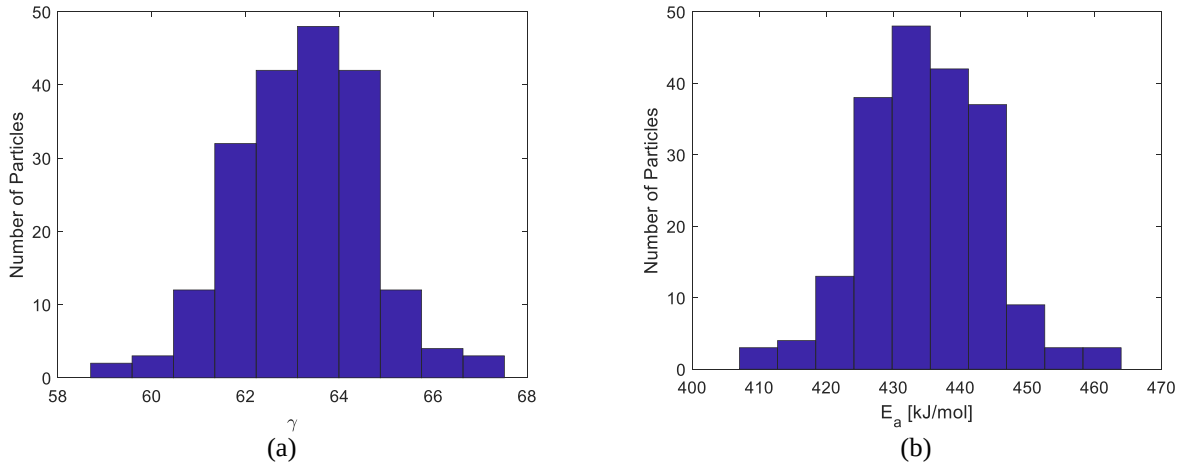


Figure 7. Histograms of the thermal damage parameters: a) $\gamma$; b) $E_a$ [kJ/mol].

The estimated position of the thermal decomposition front, obtained with the calibrated parameters, is shown by the yellow line in Fig. 8, giving a distance of 6 mm from the top surface, which corresponds to a temperature of 71.85 °C.

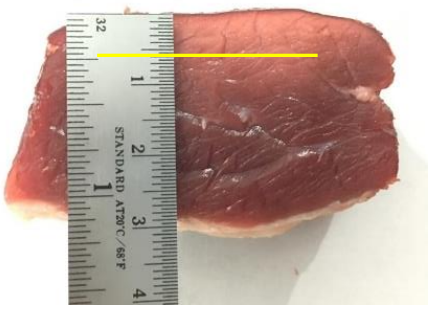

Figure 8. Thermal damaged estimated position by the calibrated parameters.

## 6. CONCLUSIONS

In this work, a sample of a biological tissue was heated by an external radiating source. The goal of this work was to reproduce numerically the experimental results of the temperature at the top and bottom surfaces of the sample. In order to do that, it was necessary to estimate the transient uniform heat flux imposed by the electrical radiator. A second experiment was then performed with a Plexiglas plate with known properties, in order to estimate the imposed heat flux with the MCMC method. The estimated heat flux was then used to estimate the thermal conductivity parameters, the heat transfer coefficient and the global heat transfer coefficient, by also using the MCMC method. Estimated and measured temperatures at the heated surface differ by 5 % at most. The ABC SMC algorithm was then applied to estimate the parameters of the Arrhenius thermal damage model, with the measurement of the thermal damage position at the final time of the experiment. By using the parameters estimated in this work, the thermal decomposition region within the tissue was appropriately predicted with the mathematical model.

## 7. ACKNOWLEDGEMENTS

The authors are thankful for the support provided by Conselho Nacional de Desenvolvimento Científico e Tecnológico (CNPq); Coordenação de Aperfeiçoamento de Pessoal de Nível Superior - Brasil (CAPES) - Finance Code 001; Fundação Carlos Chagas Filho de Amparo à Pesquisa do Estado do Rio de Janeiro, Brasil.

## 8. REFERENCES

Abraham, J.P., Plourde, B.D., Vallez, L.J., Nelson-Cheeseman, B.B., Stark, J.R., Sparrow, E.M. and Gorman, J.M., 2018. "Skin burns". In Shrivastava, D. (Ed.), *Theory and Applications of Heat Transfer in Humans*, pp. 723–739, John Wiley & Sons Ltd.

Abraham, J.P., Nelson-Cheeseman, B.B., Sparrow, E., Wentz, J.E., Gorman, J.M. and Wolf, S.E., 2016. "Comprehensive method to predict and quantify scald burns from beverage spills". *International Journal of Hyperthermia*, Vol. 32, No. 8, pp. 900–910.

Abreu, L.A.S., Orlande, H.R.B., Colaço, J.M., Kaipio, J., Kolehmainen, V., Pacheco, C.C. and Cotta, R.M., 2018. "Detection of contact failures with the Markov chain Monte Carlo method by using integral transformed measurements". *International Journal of Thermal Sciences*, Vol. 132, pp. 486–497.

Atiyeh, B.S., Gunn, S.W.A. and Hayek, S.N., 2007. "Military and civilian burn injuries during armed conflicts". *Annals of Burns and Fire Disasters*. Vol. 20, No. 4, pp. 203–215.

Hastings, W.K., 1970. "Monte Carlo sampling methods using Markov chains and their applications". *Biometrika*, Vol. 57, pp. 97–109.

Henriques, F.C. Jr., 1947. "Studies of thermal injury. V. The predictability and the significance of thermally induced rate processes leading to irreversible epidermal injury". *Archives of Pathology*, Vol. 43, No. 5, pp. 489–502.

Henriques, F.C. Jr. and Moritz, A.R., 1947. "Studies of thermal injury. I. The conduction of heat to and through skin and the temperatures attained therein. A theoretical and an experimental investigation". *American Journal of Pathology*. Vol. 23, No. 4, pp. 531–549.

Metropolis, N., Rosenbluth, A.W., Rosenbluth, M.N., Teller, A.H. and Teller, E., 1953. "Equation of state calculations by fast computing machines". *The Journal of Chemical Physics*, Vol. 21, No. 6, pp. 1087–1092.

Moritz, A.R., 1947. "Studies of thermal injury. III. The pathology and pathogenesis of cutaneous burns. An experimental study". *American Journal of Pathology*, Vol. 23, No. 6, pp. 915–941.

Moritz, A.R. and Henriques, F.C. Jr., 1947. "Studies of thermal injury. II. The relative importance of time and surface temperature in the causation of cutaneous burns". *American Journal of Pathology*, Vol. 23, No. 5, pp. 695–720.

Ozisik, M.N., Orlande, H.R.B., Colaço, M.J. and Cotta, R.M., 2017. *Finite Difference Methods in Heat Transfer*. Boca Raton: CRC Press, 2nd edition.

Patankar, S.V., 1980. *Numerical Heat Transfer and Fluid Flow*. Hemisphere Publishing Corporation.

Pennes, H.H., 1948. "Analysis of tissue and arterial blood temperatures in the resting human forearm". *Journal of Applied Physiology*, Vol. 1, No. 2, pp. 93–122.

Toni, T., Welch, D., Strelkowa, N., Ipsen, A. and Stumpf, M.P.H., 2009. "Approximate Bayesian computation scheme for parameter inference and model selection in dynamical systems". *Journal of the Royal Society Interface*. Vol. 6, pp. 187–202.

Valvano, J.W., 2018. "Thermal property measurements". In Shrivastava, D. (Ed.), *Theory and Applications of Heat Transfer in Humans*, pp. 333–354, John Wiley & Sons Ltd.

Valvano, J.W., 2011. "Tissue thermal properties and perfusion". In Welch, A.J. and van Gemert, M.J.C. (Eds.), *Optical-Thermal Response of Laser Irradiated-Tissue*, pp. 455–485, Springer, 2nd edition.

## 9. RESPONSIBILITY NOTICE

The authors are the only responsible for the printed material included in this paper.